Aseismic deformation of a fold-and-thrust belt imaged by synthetic aperture radar interferometry near Shahdad, southeast Iran

Eric J. Fielding* Jet Propulsion Laboratory, M.S. 300-233, California Institute of Technology, 4800 Oak Grove Drive, Pasadena, California 91109, USA
Tim J. Wright Centre for the Observation and Modelling of Earthquakes and Tectonics (COMET) and Department of Earth Sciences, University of Oxford, Parks Road, Oxford OX1 3PR, UK
Jordan Muller Department of Geological and Environmental Sciences, Stanford University, Stanford, California 94305, USA
Barry E. Parsons Centre for the Observation and Modelling of Earthquakes and Tectonics (COMET) and Department of Earth Sciences, University of Oxford, Parks Road, Oxford OX1 3PR, UK
Richard Walker Centre for the Observation and Modelling of Earthquakes and Tectonics (COMET) and Department of Earth Sciences, Bullard Laboratories, University of Cambridge, Madingley Road, Cambridge CB3 0EZ, UK

ABSTRACT

At depth, many fold-and-thrust belts are composed of a gently dipping, basal thrust fault and steeply dipping, shallower splay faults that terminate beneath folds at the surface. Movement on these buried faults is difficult to observe, but synthetic aperture radar (SAR) interferometry has imaged slip on at least 600 km^2 of the Shahdad basal-thrust and splay-fault network in southeast Iran. Approximately 70 mm of thrust motion on the 8°-dipping Shahdad basal thrust occurred 8–30 km to the east of the 14 March 1998 Fandoqa earthquake (M_w = 6.6) that involved 1.6 m of oblique (strike slip and normal slip) displacement on a steeply dipping fault. That earthquake transferred stress to the Shahdad basal thrust and associated splays, triggering slip either immediately or in the following six months. Modeling shows that, to produce the observed surface deformation, the Shahdad faults must have accommodated a nearly complete release of the shear stress increase. This could be due to either low friction on the faults or deformation throughout a wedge of material that is everywhere close to failure. The anomalously small magnitude of displacement on the Shahdad basal thrust and splay faults compared to the area of slip suggests a slip mechanism that is likely aseismic.

Keywords: fold-and-thrust belts, faults, synthetic aperture radar interferometry, satellite measurements, elastic modeling.

INTRODUCTION

Thin-skinned fold-and-thrust belts often form within sequences of horizontally compressed, flat-lying layers of sedimentary rock. Nearly horizontal thrust faults in layers with low strength detach steeper splay faults and cause folding in the overlying rock layers. Many studies have used laboratory sand-box models to study the behavior of these fold-and-thrust belts (e.g., Cotton and Koyi, 2000; Davis et al., 1983), but full-size systems are difficult to investigate because of the geologic time scales of the deformation. The 20 September 1999 (M_w = 7.6) earthquake at Chi-Chi, Taiwan, ruptured a splay thrust, the Chelungpu fault (Kao and Chen, 2000), within a type example of a fold-and-thrust belt (Davis et al., 1983), but elsewhere there are few direct observations of present deformation within fold-and-thrust belts on land. Questions remain about how the deformation occurs: is movement on the basal thrust and the splay faults simultaneous, and does it occur in earthquakes or aseismically?

On 14 March 1998, the moderately large Fandoqa earthquake (M_w = 6.6) struck a sparsely inhabited area in southeast Iran (Fig. 1) (Berberian et al., 2001), rupturing part of the Gowk fault zone, a predominantly right lateral strike-slip zone (Walker and Jackson, 2002). A section of a nearby shallow (between 1 and 4 km beneath the surface) and shallowly dipping (6°) thrust fault also moved during a 2 yr interval (including the Fandoqa earthquake; Berberian et al., 2001). We analyze this shallow thrust motion and its driving forces in this paper. The observed amount of slip is small (average 70 mm) but affected a large area (22 km across and 29 km along strike), equivalent to a moment magnitude M_w = 6.0 (1.5×10^{18} N·m) if released seismically, but it generated no detectable seismic signal (Berberian et al., 2001).

The Gowk fault system (Walker and Jackson, 2002) extends along the east edge of the 2-km-high Iranian plateau (Fig. 1). East of the Gowk fault and adjacent mountains are Neogene molasse deposits (well-stratified gypsiferous marl, sandstone, and conglomerate) estimated to be >3500 m thick (Berberian et al., 2001), whose surface slopes 2.6° into the Lut depression (Fig. 1). A set of three to five narrow ridges caused by active folds and faults break the slope and form the Shahdad fold-thrust belt (Fig. 1; Walker and Jackson, 2002). Based on analogies to other fold-thrust belts and the results described here, we infer a gently southwest dipping thrust beneath the 25-km-wide belt, probably a detachment at the base of the Neogene sedimentary rocks, that we call the Shahdad basal thrust. There may be a thin layer of evaporites that lubricates the detachment, but there is no evidence here for a thick salt unit like that beneath the Zagros fold-and-thrust belt. We also infer, from analogues and our data, steeper thrust faults that splay upward from the basal thrust but do not reach the surface, instead ending in blind thrusts beneath each of the folds. Thrust displacement along a reduced-friction basal detachment allows the wedge above it and east of the Gowk fault to move eastward and thicken, driven partly by the steep topographic gradient from the plateau to the Lut depression (Walker and Jackson, 2002). The surface slope and basal thrust dip of this wedge are similar to those of other wedges (Davis et al., 1983) (Fig. 1B).

SYNTHETIC APERTURE RADAR INTERFEROMETRY AND KINEMATIC FAULT MODELS

We formed interferograms from two pairs of European Remote Sensing satellite synthetic aperture radar (SAR) images that span the 1998 Fandoqa earthquake and one pair covering a half-year interval after the earthquake (Table DR1; details of the SAR interferometry data, processing, inversions, and modeling).[1] Despite time intervals to 3 yr, the

*E-mail: Eric.J.Fielding@jpl.nasa.gov.

[1]GSA Data Repository item 2004092, Appendix DR1 and Table DR1, and Figures DR1–DR4, with details of the synthetic aperture radar interferometry data, processing, inversions and modeling, is available online at www.geosociety.org/pubs/ft2004.htm, or on request from editing@geosociety.org or Documents Secretary, GSA, P.O. Box 9140, Boulder, CO 80301-9140, USA.

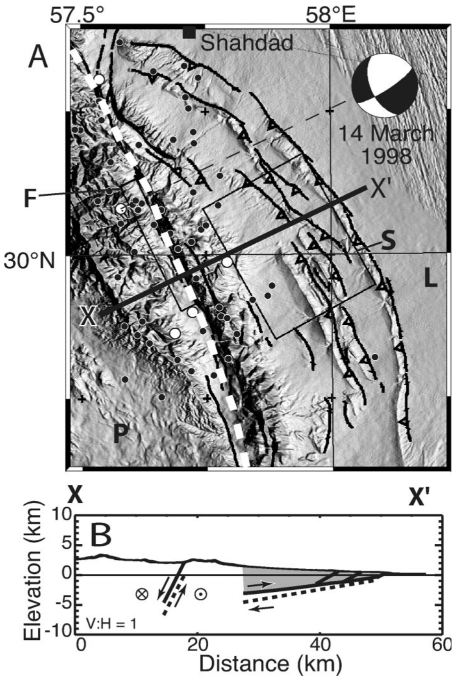

Figure 1. A: Shaded relief topographic map of Shahdad area with active faults (medium black lines) (Walker and Jackson, 2002), X-X′ profile location (thick black line), moderate earthquakes (black filled circles), four large earthquakes since 1981 (white filled circles), and fault-plane solution (upper right) for Fandoqa earthquake (Berberian et al., 2001). Rectangles with thin black lines are Fandoqa rupture (F) and Shahdad basal-thrust (S) dislocations shown in other figures. Thick dashed white line—Gowk fault zone; P—central Iranian plateau; L—Lut block. B: Topographic profile and depth cross section of Fandoqa main shock, Shahdad basal thrust, and splay slip planes. Solid lines show positions of fault planes from inversion after adjustment for topography; dashed lines are unadjusted. Gray fill shows Shahdad thrust wedge.

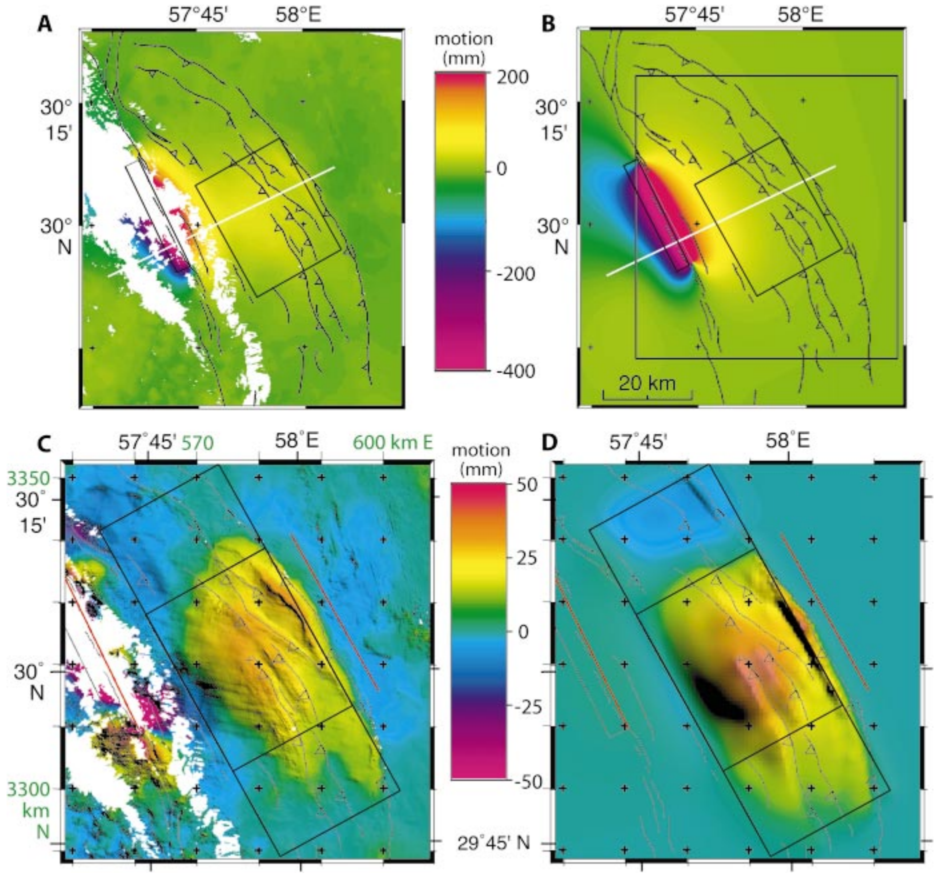

Figure 2. A: Average of two interferograms, converted to radar range change (motion in radar line of sight) in millimeters. Faults (black lines) and profile location (white line) as in Figure 1A. Rectangles (thin lines) show surface locations of Fandoqa and Shahdad basal-thrust dislocation models. B: Surface deformation from Fandoqa main-shock elastic model, shown as radar range change. Large rectangle outlines area shown in C and D. C: Residual interferogram after subtracting Fandoqa main shock model shown in B. Note that color scale and area are different from A and B. Green labels are Universal Transverse Mercator zone 40 coordinates and tics are every 10 km. Thin red lines show updip projections of Fandoqa and Shahdad basal thrust to surface. Larger rectangle shows extended Shahdad basal thrust used in distributed slip inversion (Fig. 3) and Poly3D (Fig. 4). D: Surface deformation predicted by slip model of Shahdad basal thrust and splays shown in Figure 4, projected into radar line of sight. Same area and colors as C.

coherence of the interferograms is excellent due to the lack of vegetation in this arid region (Fig. 2). We used an elastic half-space model (Okada, 1985) and an inversion procedure to determine an optimum dislocation for the Fandoqa main shock fitting the average of the two coseismic interferograms (Wright et al., 1999). This simple elastic model with one dislocation patch having constant slip of 1.7 m reasonably fits the observed radar range changes in the area of the Fandoqa main shock (Fig. 2B) and agrees with a seismic waveform solution (Berberian et al., 2001) (for the inversion details, see footnote 1).

When we subtract the range change of the Fandoqa main-shock model from the interferogram, a roughly rectangular 20 × 30 km area of decreased range remains over the central Shahdad fold-and-thrust belt east of the Fandoqa earthquake rupture (Fig. 2C). The 20–40 mm range decrease in this area means that the ground surface within the patch moved toward the radar, eastward and upward. This cannot be due to errors in the elevation model used in processing because it appears the same on both interferograms (1 and 2), despite the difference in their sensitivity to elevation (Table DR1; see footnote 1), and because the northern and southern boundaries of the patch are not at any topographic feature. The similarity of the Shahdad signature on two completely independent interferograms also indicates that the feature cannot be an atmospheric effect. We performed a second inversion for an elastic dislocation (Okada, 1985) fitting the Shahdad range change (Fig. 2C), holding the dislocation of the Fandoqa main shock fixed and constraining the rake to 90° with all other parameters free (see footnote 1 for more details). The result is a large patch of slip on a shallow and shallowly dipping surface that we interpret as the basal thrust of the Shahdad thrust belt (Fig. 1B). This rectangle is 22 × 29 km and dips southwestward at 9.7° beneath the surface of the elastic half-space (6.1° from Earth horizontal), with uniform thrust slip of 70 mm.

To determine the distribution of slip on the Shahdad basal thrust, we took the derived rectangle and extended it in all four directions to match the length and width of the Shahdad fold-and-thrust belt. We inverted for dip slip on 4 × 4 km patches, fixing the geometry (Fig. 3). Even though the extended rectangle could allow slip beyond the original rectangle, the distributed slip inversion keeps most of the slip in the same area with a very sharp boundary on the southwest (downdip) side. The uncertainty in the measurements varies, but is close to 5 mm for most of the area (see Data Repository text and Fig. DR4 for details, footnote 1).

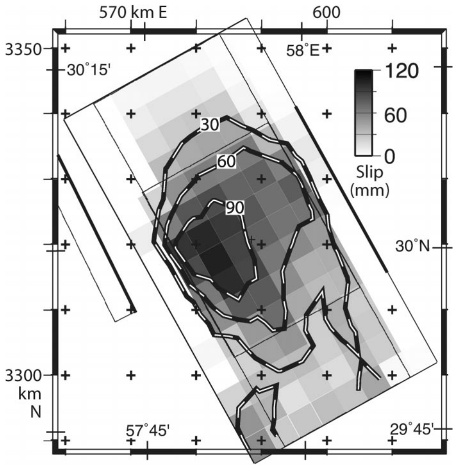

Figure 3. Distribution of slip on Shahdad basal thrust calculated from average of interferograms (Fig. 2C). Gray levels and contours show dip-slip motion in millimeters. Thick black lines show updip projections of constant-slip rectangle solutions to surface. Thin lines show vertical projections of Fandoqa rupture and Shahdad basal thrust: constant-slip rectangle (shown in Figs. 1 and 2), extended rectangle used in this distributed slip inversion, and narrower rectangle used in boundary element model (Fig. 4). Other symbols as in Figure 2C.

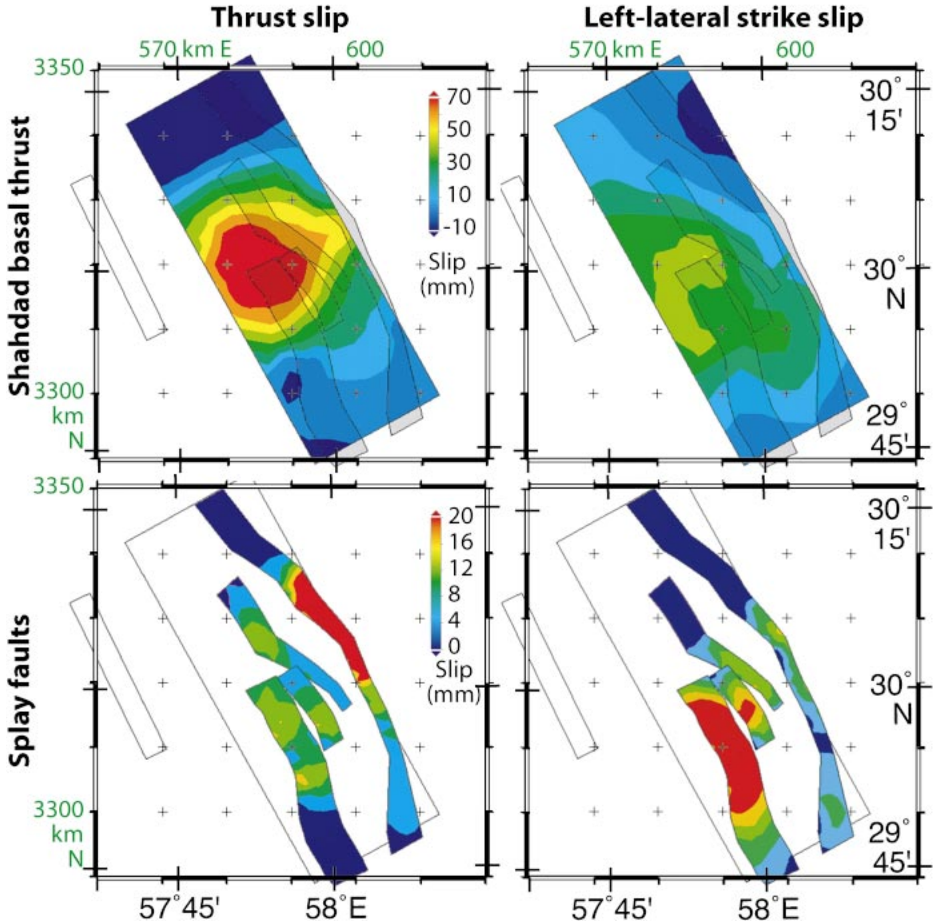

Figure 4. Slip solution from boundary element model (Poly3D) in map view. Top row shows slip on basal thrust, bottom row shows slip on splay faults. Left column shows dip-slip component, right column shows strike-slip component. Labels are similar to those in Figure 2C.

STRESS MODELING

Stress transfer has been invoked to explain slip on faults adjacent to one or more earthquakes (Toda and Stein, 2002). The shear stress in the thrust direction on the Shahdad basal thrust increased by at least 0.02 MPa (0.2 bar) due to the Fandoqa earthquake in the area where we observe aseismic slip (Fig. 3), similar to the stress increase that has been shown to trigger earthquakes (Stein, 1999). Because of the very shallow dip of the Shahdad basal thrust, there is almost no change in the normal stress. Coulomb stress changes (Stein, 1999) are then equal to shear-stress changes.

We use an elastic half-space boundary element model called Poly3D (Thomas, 1993) to calculate slip on the Shahdad faults due to the stress perturbation from the Fandoqa earthquake, assuming complete release of the applied shear-stress changes. We find that the Shahdad décollement motion derived from the InSAR (SAR interferometry) inversion (Fig. 3) almost exactly matches the slip predicted by the boundary element model (BEM) (Fig. 4). The BEM also predicts a substantial amount of left-lateral slip on the basal thrust and splays, but strike-slip displacements are not well constrained by the InSAR result because the single radar look direction is nearly normal to the faults. This apparent left-lateral slip in the BEM is due to the simplified assumption of no preexisting far-field tectonic stress. Including a preexisting right-lateral shear stress from ongoing deformation on the major Gowk fault zone would counteract the left-lateral stress change from the Fandoqa event. Forward modeling of the surface deformation from the BEM result (Fig. 2D) shows that the predicted range change fits the interferogram nearly as well as the thrust-only inversion model (Fig. 3). The short-wavelength (2–4 km) features observed on the residual interferogram (Fig. 2C) also are well matched by slip on the BEM splay faults (Figs. 2D and 4).

DISCUSSION AND CONCLUSIONS

The long time interval ($\sim$3 yr) of the interferograms does not constrain the timing of the Shahdad deformation, but the observable similarity of the measured slip distribution with the slip predicted by the BEM is strong evidence that the static stress changes due to the Fandoqa earthquake caused the slip on the basal thrust and splays. The Shahdad deformation signal is almost the same on two interferograms that include 6 and 12 months after the Fandoqa earthquake (1 and 2, Table DR1; see footnote 1), so the bulk of the deformation happened within 6 months. This inference is confirmed by the lack of measurable radar range change on interferogram 3 from September 1998 to March 1999. A somewhat similar aseismic slip event was detected by ground geodetic instruments beneath Kilauea volcano, with a duration of $\sim$36 h and magnitude of 87 mm at a depth of 4.5 km (Cervelli et al., 2002), so the Shahdad event might have had a similar duration.

The earthquake scaling relationships of Wells and Coppersmith (1994) predict a magnitude **M** of 6.9 for an earthquake with a fault rupture area of 642 km^2, the area of slip on the Shahdad basal thrust. The observed 70 mm average displacement is more than an order of magnitude smaller than the displacement of 0.74 m necessary to produce an **M** = 6.9 earthquake with that rupture area. This comparison indicates that the elastic strain released by the Shahdad basal thrust and splay-fault slip was much smaller than events that typically generate seismic waves. Previous attempts to find the Shahdad basal slip in the seismic waveforms from the Fandoqa earthquake were unable to find any evidence of it

(Berberian et al., 2001), although it may be hidden by the larger waves of the main shock.

Field observations of triggered slip have been made previously on thrust faults adjacent to earthquakes on large active strike-slip faults, including the 1957 Mongolia earthquake (Bayasgalan et al., 1999) and the 1989 Loma Prieta (California) earthquake (Bürgmann et al., 1997; Langenheim et al., 1997). InSAR has also been used to detect triggered slip on strike-slip faults (Fialko et al., 2002; Wright et al., 2001). This study presents the first demonstration of triggered slip on a shallow and gently dipping thrust and associated splay faults in a fold-and-thrust belt.

Despite the inferred presence of gently dipping and active thrust faults in many locations, the lack of recorded earthquakes on such thrusts at shallow depths ($<$4 km) further suggests that these structures are aseismic. In many places, earthquakes occur on steeper ramp sections of the basal thrust faults, but not on the adjacent flat sections: (1) The Chi-Chi earthquake ruptured a steeper ($\sim$20° dip) splay (Kao and Chen, 2000). Geodetic measurements of postseismic deformation in the area of the Chi-Chi earthquake suggest that some of the gently dipping décollement slipped aseismically in the months after the large earthquake (Hsu et al., 2002). (2) Some large shallowly dipping thrusts extend from shallow depths to mid-crustal depths, such as the Main Himalayan thrust (Pandey et al., 1999; Yeats and Lillie, 1991) and many subduction-zone thrusts (Shipley et al., 1994). On these large thrusts, great earthquakes are believed to occur on the deeper part of the thrust and propagate slip up to the shallow parts (Pandey et al., 1999; Yeats and Lillie, 1991). Between large events, there is ongoing seismic activity around the deeper parts of the thrust but little activity on the shallow, flat parts (Pandey et al., 1999). This finding suggests that the shallow parts of gently dipping thrusts are either (1) décollements that have very low friction levels and do not accumulate elastic stress, or (2) moderate-friction detachments where the elastic stress is at a threshold for failure so that any stress increment is released. The shallow slip that we describe here is consistent with both of these views of shallow and gently dipping thrusts because the slip seems to have released the stress imposed on the basal thrust aseismically. If all or most of the motion on the Shahdad basal thrust and splays is aseismic, then there is little seismic risk associated with these faults. If displacement on other shallow and gently inclined thrust faults is similar, this behavior has important implications for seismic hazard evaluations, because shallow thrust and splay faults are believed to be present beneath the city of Los Angeles (Davis and Namson, 1994), the Santa Clara valley (Bürgmann et al., 1997; Langenheim et al., 1997), west-central Taiwan (Kao and Chen, 2000), and other areas of active thrust faults.

ACKNOWLEDGMENTS

We thank J.A. Jackson, P. Lundgren, and E. Ivins for discussions and R. Bürgmann for a helpful review. European Remote Sensing synthetic aperture radar data are copyrighted and courtesy of the European Space Agency under projects AO3-213 and AO3-371. Part of this work was performed at the Jet Propulsion Laboratory, California Institute of Technology, under contract with the U.S. National Aeronautics and Space Administration. Centre for the Observation and Modelling of Earthquakes and Tectonics (COMET) is an Earth Observation Centre supported by the UK National Environmental Research Council (NERC). This work was supported by a NERC postdoctoral research fellowship (Wright) and the Stanford Rock Fracture Project (Muller). Some figures were prepared with the Generic Mapping Tools package (Wessel and Smith, 1998).

REFERENCES CITED

Bayasgalan, A., Jackson, J.A., Ritz, J.-F., and Carretier, S., 1999, ''Forebergs'', flower structures, and the development of large intracontinental strike-slip faults: The Gurvan Bogd fault system in Mongolia: Journal of Structural Geology, v. 21, p. 1285–1302.

Berberian, M., Jackson, J.A., Fielding, E.J., Parsons, B.E., Priestley, K., Qorashi, M., Talebian, M., Walker, R., Wright, T.J., and Baker, C., 2001, The 1998 March 14 Fandoqa earthquake (M_w 6.6) in Kerman province, southeast Iran: Re-rupture of the 1981 Sirch earthquake fault, triggering of slip on adjacent thrusts and the active tectonics of the Gowk fault zone: Geophysical Journal International, v. 146, p. 371–398.

Bürgmann, R., Segall, P., Lisowski, M., and Svarc, J., 1997, Postseismic strain following the 1989 Loma Prieta earthquake from GPS and leveling measurements: Journal of Geophysical Research, v. 102, no. B3, p. 4933–4955.

Cervelli, P., Segall, P., Johnson, K., Lisowski, M., and Miklius, A., 2002, Sudden aseismic fault slip on the south flank of Kilauea volcano: Nature, v. 415, p. 1014–1018.

Cotton, J.T., and Koyi, H.A., 2000, Modeling of thrust fronts above ductile and frictional detachments: Application to structures in the Salt Range and Potwar Plateau, Pakistan: Geological Society of America Bulletin, v. 112, p. 351–363.

Davis, D., Suppe, J., and Dahlen, F.A., 1983, Mechanics of fold-and-thrust belts and accretionary wedges: Journal of Geophysical Research, v. 88, no. B2, p. 1153–1172.

Davis, T.L., and Namson, J.S., 1994, A balanced cross-section of the 1994 Northridge earthquake, southern California: Nature, v. 372, p. 167–169.

Fialko, Y., Sandwell, D., Agnew, D., Simons, M., Shearer, P., and Minster, B., 2002, Deformation on nearby faults induced by the 1999 Hector Mine earthquake: Science, v. 297, p. 1858–1862.

Hsu, Y.-J., Bechor, N., Segall, P., Yu, S.-B., Kuo, L.-C., and Ma, K.-F., 2002, Rapid afterslip following the 1999 Chi-Chi, Taiwan earthquake: Geophysical Research Letters, v. 29, p. 1754, doi: 10.1029/2002GL014967.

Kao, H., and Chen, W.-P., 2000, The Chi-Chi earthquake sequence: Active, out-of-sequence thrust faulting in Taiwan: Science, v. 288, p. 2346–2349.

Langenheim, V.E., Schmidt, K.M., and Jachens, R.C., 1997, Coseismic deformation during the 1989 Loma Prieta earthquake and range-front thrusting along the southwestern margin of the Santa Clara Valley, California: Geology, v. 25, p. 1091–1094.

Okada, Y., 1985, Surface deformation due to shear and tensile faults in a half-space: Seismological Society of America Bulletin, v. 75, p. 1135–1154.

Pandey, M.R., Tandukar, R.P., Avouac, J.P., Vergne, J., and Héritier, T., 1999, Seismotectonics of the Nepal Himalaya from a local seismic network: Journal of Asian Earth Sciences, v. 17, p. 703–712.

Shipley, T.H., Moore, G.F., Bangs, N.L., Moore, J.C., and Stoffa, P.L., 1994, Seismically inferred dilatancy distribution, Northern Barbados Ridge decollement—Implications for fluid migration and fault strength: Geology, v. 22, p. 411–414.

Stein, R.S., 1999, The role of stress transfer in earthquake occurrence: Nature, v. 402, p. 605–609.

Thomas, A.L., 1993, Poly3D: A three-dimensional, polygonal element, displacement discontinuity boundary element computer program with applications to fractures, faults, and cavities in the Earth's crust [M.S. thesis]: Stanford, California, Stanford University, 221 p.

Toda, S., and Stein, R.S., 2002, Response of the San Andreas fault to the 1983 Coalinga-Nuñez earthquakes: An application of interaction-based probabilities for Parkfield: Journal of Geophysical Research, v. 107, no. B6, p. 2126.

Walker, R., and Jackson, J.A., 2002, Offset and evolution of the Gowk fault, S.E. Iran: A major intra-continental strike-slip system: Journal of Structural Geology, v. 24, p. 1677–1698.

Wells, D.L., and Coppersmith, K.J., 1994, New empirical relationships among magnitude, rupture length, rupture width, rupture area, and surface displacement: Seismological Society of America Bulletin, v. 84, p. 974–1002.

Wessel, P., and Smith, W.H.F., 1998, New, improved version of the Generic Mapping Tools released: Eos (Transactions, American Geophysical Union), v. 79, p. 579.

Wright, T.J., Parsons, B.E., Jackson, J.A., Haynes, M., Fielding, E.J., England, P.C., and Clarke, P.J., 1999, Source parameters of the 1 October 1995 Dinar (Turkey) earthquake from SAR interferometry and seismic bodywave modelling: Earth and Planetary Science Letters, v. 172, p. 23–37.

Wright, T.J., Fielding, E.J., and Parsons, B.E., 2001, Triggered slip: Observations of the 17 August 1999 Izmit (Turkey) earthquake using radar interferometry: Geophysical Research Letters, v. 28, p. 1079–1082.

Yeats, R.S., and Lillie, R.J., 1991, Contemporary tectonics of the Himalayan frontal fault system—Folds, blind thrusts and the 1905 Kangra earthquake: Journal of Structural Geology, v. 13, p. 215–225.

Manuscript received 5 January 2004
Revised manuscript received 8 March 2004
Manuscript accepted 11 March 2004

Printed in USA